Relationship Between Drusen Height and OCT Biomarkers of Atrophy in Non-Neovascular AMD

Adrian Au,[1] Ahmad Santina,[1] Neda Abraham,[1] Miri Fogel Levin,[1] Giulia Corradetti,[2] SriniVas Sadda,[2] and David Sarraf[1,3]

[1]Retinal Disorders and Ophthalmic Genetics Division, Stein Eye Institute, University of California Los Angeles, Los Angeles, California, United States
[2]Doheny Eye Institute, Department of Ophthalmology, University of California, Los Angeles, Los Angeles, California, United States
[3]Greater Los Angeles VA Healthcare Center, Los Angeles, California, United States

Correspondence: David Sarraf, Retinal Disorders and Ophthalmic Genetics Division, Stein Eye Institute, University of California Los Angeles, 100 Stein Plaza, Los Angeles, CA 90095, USA; sarraf@jsei.ucla.edu.

Received: April 25, 2022
Accepted: September 9, 2022
Published: October 28, 2022

Citation: Au A, Santina A, Abraham N, et al. Relationship between drusen height and OCT biomarkers of atrophy in non-neovascular AMD. *Invest Ophthalmol Vis Sci.* 2022;63(11):24. https://doi.org/10.1167/iovs.63.11.24

Purpose. To determine if increasing drusen height correlates with predictive optical coherence tomography (OCT) biomarkers of atrophy.

Methods. Retrospective cross-sectional study that enrolled patients with drusen associated with intermediate AMD. Macular drusen were classified as small, intermediate, large, or very large based on OCT quartile measurement of height. Drusen diameter was also tabulated. The presence and localization of the OCT biomarkers of atrophy were assessed: disruption of the external limiting membrane and ellipsoid zone, intraretinal hyper-reflective foci, RPE disruption, choroidal hypertransmission, and presence of hyporeflective cores. Predictive OCT biomarkers of atrophy were correlated with drusen height.

Results. A total of 155 eyes from 104 patients met the inclusion and exclusion criteria. The mean age was 75.7 ± 8.7 years, and patients were predominantly female (74.0%). The mean visual acuity was logMAR 0.2 ± 0.2 (Snellen equivalent 20/32). The average drusen height was 134.6 ± 107.5 µm and the greatest horizontal diameter was 970.7 ± 867.4 µm. Disruption of the external limiting membrane and ellipsoid zone, RPE thickening or thinning, intraretinal hyper-reflective foci, choroidal hypertransmission, and presence of hyporeflective cores ($P < 0.05$) were more common in eyes with large drusen and very large drusen versus small or intermediate drusen. All biomarkers were positively correlated with drusen height. OCT biomarkers of atrophy were predominantly located at the apex of the drusen.

Conclusions. Predictive OCT biomarkers of atrophy, specifically signs of RPE breakdown and disruption, occur more commonly in large or very large drusen, especially in drusen with greater height and separation of the RPE from the underlying choroid.

Keywords: AMD, atrophy, OCT, druse, drusen

Drusen represent the defining feature of non-neovascular AMD and are a significant risk factor for the development of geographic atrophy and macular neovascularization. The relative risk of geographic atrophy was determined by the Age-related Eye Disease Studies (AREDS), which concluded that larger drusen (>125 µm) or drusenoid pigment epithelial detachments (PED; >350 µm), based on color fundus photography diameter measurements, were at higher risk of progression to atrophy.[1–3]

Optical coherence tomography (OCT) biomarkers of atrophy are important to accurately predict the progression to geographic atrophy and complete RPE and outer retinal atrophy (cRORA). OCT predictors of atrophy include intraretinal hyperreflective foci, focal RPE thickening, and choroidal hypertransmission.[4] These features are the earliest signs of RPE impairment and disruption.[5] In a recent study evaluating the presence of subretinal fluid in non-neovascular AMD, Hilely et al.[6] proposed that RPE pump failure owing to decreased choroidal perfusion associated with large drusen can explain the development of overlying subretinal fluid. This finding suggests that as the height of the drusen increases the separation of the RPE from the underlying choroid, RPE failure may ensue and can be detected as early signs of atrophy on OCT.

Traditionally, large drusen at high risk for developing atrophy are classified on the basis of diameter as measured with color fundus photography.[1–3] Although few studies have shown that drusen height is a risk factor for developing atrophy, they do not formally quantitate this risk with OCT height or correlate this risk with recently codified predictive OCT biomarkers of atrophy.[3,7] Herein, we performed an exploratory study designed to correlate the increasing height of drusen, and specifically the distance between the choriocapillaris and the RPE, with the presence of OCT predictive biomarkers of atrophy.

Methods

This retrospective cross-sectional study was approved by the Institutional Review Board at the University of California, Los Angeles, and adhered to the Health Insurance Portability and Accountability Act and was performed in accordance with the Declaration of Helsinki. The OCT images of patients being evaluated and treated for non-neovascular AMD by two tertiary retina specialists (DS, SS) were collected and analyzed.

Patients over the age of 60 with a diagnosis of non-neovascular intermediate AMD (at the time of analysis) and with high-quality OCT volume scans illustrating the presence of macular drusen of any size at any follow-up were included for evaluation between October 2009 and July 2021. Exclusion criteria included any history of anti-VEGF injection and any clinical, OCT, or OCT angiography evidence of macular neovascularization such as fluid, hemorrhage, or subretinal hyperreflective material. Patients with OCT findings of cRORA as defined by the CAM Report 3 were also excluded.[8] Eyes exhibiting predominantly reticular pseudodrusen or subretinal drusenoid deposits or cuticular drusen were also excluded. Cases with evidence of fluid, resulting from retinal vascular disease (e.g., diabetic retinopathy, retinal vein occlusions) or from tractional epiretinal membranes were also not included in the analysis. All patients underwent a complete ophthalmologic examination, including a dilated fundus examination. Heidelberg Spectralis OCT (Heidelberg Engineering Inc, Heidelberg, Germany) or Cirrus HD-OCT (Carl Zeiss Meditec, Dublin, CA) was performed on all patients and OCT images were analyzed. Heidelberg Spectralis scans were 20° × 20° and were acquired using a 97 B-scan volume dataset with an ART mean function of 10 per B scan or were 30° × 20° with a volume dataset of 25 B-scans and an ART mean function of 15. Cirrus HD-OCT scans were acquired in a 128 × 512 cube with 128 B-scans and 512 A-scans in a 6 × 6-mm cube.

OCT images were selected based on the presence of drusen, quality of the image, and clear identification of the scleral–choroidal junction (either with or without the use of enhanced depth imaging). In the case of multiple follow-up visits, the earliest OCT volume dataset with visible drusen and the aforementioned inclusion and exclusion criteria was selected for analysis. Both eyes were eligible for enrollment. Patients who developed atrophy or neovascularization were still included if the OCT scans were analyzed before the development of atrophy or neovascularization.

OCT images were exported to FIJI-ImageJ (1.52; http://imagej.nih.gov/ij/; provided in the public domain by the National Institutes of Health, Bethesda, MD, USA) for quantitative analysis.[9] The largest druse in the available macular volume cube was used to compare across patients. Images were scaled according to the scale bar provided on 1:1 micron exported Heidelberg or Cirrus scans. The scale was adjusted to either the vertical scale bar for vertical measurements (e.g., drusen height and choroidal thickness) and the horizontal scale bar for horizontal measurements (e.g., greatest horizontal diameter [GHD]). However, no adjustments were made according to the ocular biometry of the OCT images. Therefore, horizontal measurements may represent nominal dimensions. The maximum height of drusen was measured from Bruch's membrane to the inner border of the RPE. The GHD of the drusen was measured as the longest width of the drusen from the inner borders of the RPE on cross-sectional OCT. Choroidal thickness was measured from the Bruch's membrane to the scleral–choroidal junction, just beneath the drusen at a point corresponding with its apex.

Eyes were categorized based on drusen height and divided quartiles for analysis. Small drusen were defined as the smallest 25% of total drusen by height, intermediate drusen were defined as the intermediate 26% to 50% of total drusen by height, large drusen were defined as the 51% to 75% of total drusen by height, and very large drusen were defined as the largest 25% of total drusen by height. To control for differences in baseline severity of AMD and choroidal thickness, control drusen were selected in the same eye. The control druse was selected as the largest non-contiguous druse that was at least 1000 microns away from the largest druse.

A qualitative analysis of predictive OCT biomarkers of atrophy were defined as described in the CAM Report 5.[4] Two graders were used to confirm each qualitative measurement (AA, AS, NA, MFL). Any discrepancies were adjudicated by a senior grader (DS). Briefly these were defined as follows:

- External limiting membrane (ELM) and ellipsoid zone (EZ) disruption: Discontinuous or attenuated reflectivity of the ELM and EZ, respectively.
- RPE thickening or thinning: A consolidated hyperreflective band along the RPE appearing as a focal enlargement of the RPE band or adjacent narrowing of the RPE, respectively.
- Intraretinal hyper-reflective foci (HRF): Discrete punctate lesions with equal or greater reflectivity than that of the RPE within the retina.
- Choroidal hypertransmission: Linear and continuous vertical streaks of hyper-reflectivity extending into the choroid and obscuring the choroidal markings.
- Hyporeflective cores within drusen: Hyporeflective spaces within the sub-RPE compartment of the druse.

OCT location of the atrophic biomarkers over the RPE surface of drusen was grouped into four categories: diffuse, apex, slope, or base. Biomarkers located throughout the circumference of the RPE band of drusen were defined as diffuse. Biomarkers identified only at the peak or apical third of the drusen were defined as apex. Biomarkers located only on either side of the apex on the downslope of the drusen were defined as slope. Biomarkers found only at the base of the drusen were defined as base. Any biomarkers extending from the apex to both slopes were defined as diffuse. For hypo-reflective cores, presence of a hypo-reflective space at the apex and the base of the drusen was defined as diffuse as well.

Statistical analyses were performed using R version 3.5.0 (www.r-project.org). Categorical variables were reported as numerical counts and percentages (male, female, bilaterality, qualitative measurements), and interval variables were reported as means and standard deviations (age, visual acuity, quantitative measurements). The Kruskal–Wallis rank-sum test with the post hoc Wilcox test was performed comparing interval variables between three groups (drusen height, size, and choroidal thickness). Qualitative measurements were compared using the χ^2 test between multiple groups and post hoc χ^2 test with Bonferroni correction for subsequent pairwise analysis. Spearman's correlation and multivariate generalized mixed linear effect modelling were performed to correlate drusen height or GHD with atrophy biomarker, while controlling for codependency and bilateral enrollment. A paired t test or χ^2 test was performed between the largest and control drusen within the same eye. Cohen's kappa was used to determine

Table 1. Demographics of the Patient Cohort ($N = 155$ Eyes, 104 Patients)

	Mean ± SD or No. (%)
Age, years	75.7 ± 8.7
Sex	
Male	27 (26.0)
Female	77 (74.0)
Eye	
OD	77 (49.7)
OS	78 (50.3)
Bilateral	51 (32.9)
Visual acuity (logMAR, Snellen equivalent)	0.2 ± 0.2 (20/32)
Drusen height (µm)	134.6 ± 107.5
Drusen GHD (µm)	970.7 ± 867.4
Choroidal thickness (µm)	216.4 ± 86.6

intergrader reliability between qualitative measurements. A P value of less than 0.05 was considered statistically significant, except when Bonferroni correction was performed ($P < 0.008$; 0.05/6).

Results

Demographics

A total of 618 patients and 1236 eyes were screened. Of these, 467 eyes were identified with drusen without any presence of concurrent atrophy or neovascularization and with sufficient image quality. Of these, 155 eyes from 104 patients were analyzed without evidence of subretinal drusenoid deposits or cuticular drusen or calcific drusen. The mean age of patients was 75.7 ± 8.7 years, and the cohort was predominantly female (77/104 [74.0%]) (Table 1). There were 77 right eyes (49.7%) and 78 left eyes (50.3%), and 51 bilateral eyes (32.9%) enrolled in the study. Snellen visual acuity was available for 105 eyes and the mean visual acuity was logMAR 0.2 ± 0.2 (Snellen equivalent 20/32). The average drusen height was 134.6 ± 107.5 µm, the average drusen GHD was 970.7 ± 867.4 µm, and average choroidal thickness was 216.4 ± 86.6 µm.

Drusen Characteristics Across All Eyes

Comparisons between quantitative and qualitative measurements are summarized in Table 2. There was a statistically significant difference in drusen height between small (56.3 ± 11.8 µm), intermediate (87.1 ± 11.6 µm), large (129.8 ± 14.3 µm), and very large (265.1 ± 142.2 µm; $P < 0.001$) drusen. A post hoc Wilcox test confirmed statistical significance between all groups ($P < 0.008$) related to height with Bonferroni correction, except for small versus intermediate drusen ($P = 0.37$) and intermediate versus large drusen ($P = 0.06$). Similarly, drusen GHD was significantly different between the small (353.9 ± 209.2 µm), intermediate (725.3 ± 460.7 µm), large (884.5 ± 497.7 µm), and very large (1916.7 ± 1083.5 µm; $P < 0.001$) drusen. With post hoc Wilcox testing, statistical significance was retained between all groups except for small versus intermediate drusen ($P = 0.07$) and intermediate versus large drusen ($P = 1.0$) with conservative Bonferroni correction. There was no difference between the underlying choroidal thickness between all groups ($P = 0.53$).

Frequency and Location of OCT Biomarkers of Atrophy Across All Eyes

Early biomarkers of atrophy, specifically findings related to RPE disruption, were more common in the cohorts with large or very large drusen. Localization analyses showed that RPE-specific changes were noted more frequently at the apex, whereas non-RPE changes were less apparent (Table 3). Examples of cases are shown in Figure 1. The results are as follows.

1. ELM disruption was observed with increasing frequency in small drusen (6/39 [15.4%]), intermediate drusen (13/39 [33.3%]), large drusen (29/38 [76.3%]), and very large drusen (37/39 [94.9%]) ($P < 0.001$). The graded increase in ELM disruption was statistically significant with post hoc χ^2 testing between all cohorts except in the comparison between small versus intermediate drusen ($P = 0.07$) and large versus very large drusen ($P = 0.02$). The intergrader Cohen's kappa was 0.64 (95% confidence interval [CI], 0.55–0.71). ELM disruption was identified more frequently in a diffuse pattern (63.5% [54/85]) or originating from the apex (35.3% [30/85]).
2. EZ disruption was present in increasing frequency in the groups with small drusen (7/39 [17.9%]), intermediate drusen (18/39 [46.2%]), large drusen (33/38 [86.8%]), and very large drusen (36/39 {.;$P < 0.001$). A post hoc χ^2 test revealed that EZ loss remained statistically significant in all groups except in the comparison of large versus very large druse ($P = 0.43$). The intergrader Cohen's kappa was 0.72 (95% CI, 0.64–0.79). EZ disruption was also most frequently noted

Table 2. Comparison of Structural and Atrophy Biomarkers by All Drusen Size Across All Eyes

	Drusen				
	Small (26.5–72.5 µm) ($n = 39$)	Intermediate (72.5–106.9 µm) ($n = 39$)	Large (106.9–156.9 µm) ($n = 38$)	Very Large (>156.9 µm) ($n = 39$)	*P* Value
Drusen height (µm)	56.3 ± 11.8	87.1 ± 11.6	129.8 ± 14.3	265.1 ± 142.2	<0.001
Drusen GHD (µm)	353.9 ± 209.2	725.3 ± 460.7	884.5 ± 497.7	1916.7 ± 1083.5	<0.001
Choroidal thickness (µm)	222.7 ± 93.5	200.1 ± 85.3	209.9 ± 78.8	232.5 ± 87.9	0.53
ELM disruption	6 (15.4)	13 (33.3)	29 (76.3)	37 (94.9)	<0.001
EZ disruption	7 (17.9)	18 (46.2)	33 (86.8)	36 (92.3)	<0.001
RPE thickening or thinning	0 (0.0)	2 (5.1)	12 (31.6)	30 (76.9)	<0.001
HRF	0 (0)	2 (5.1)	7 (18.4)	23 (59.0)	<0.001
Choroidal hypertransmission	13 (33.3)	8 (20.5)	16 (42.1)	29 (74.4)	<0.001
Hyporeflective cores	0 (0.0)	0 (0.0)	0 (0.0)	5 (12.8)	0.002

Values are mean ± SD or number (%).

Investigative Ophthalmology & Visual Science

Table 3. Location of OCT Atrophy Biomarkers

	Diffuse	Apex	Slope	Base
ELM disruption ($n = 85$)	54 (63.5)	30 (35.3)	1 (1.2)	0 (0.0)
EZ disruption ($n = 94$)	53 (56.4)	39 (41.5)	2 (2.1)	0 (0.0)
RPE thickening or thinning ($n = 44$)	2 (4.5)	40 (90.9)	3 (6.8)	0 (0.0)
HRF ($n = 32$)	0 (0.0)	32 (100.0)	0 (0.0)	0 (0.0)
Choroidal hypertransmission ($n = 66$)	47 (71.2)	19 (28.8)	0 (0.0)	0 (0.0)
Hyporeflective cores ($n = 5$)	3 (60.0)	2 (40.0)	0 (0.0)	0 (0.0)

Values are number (%).

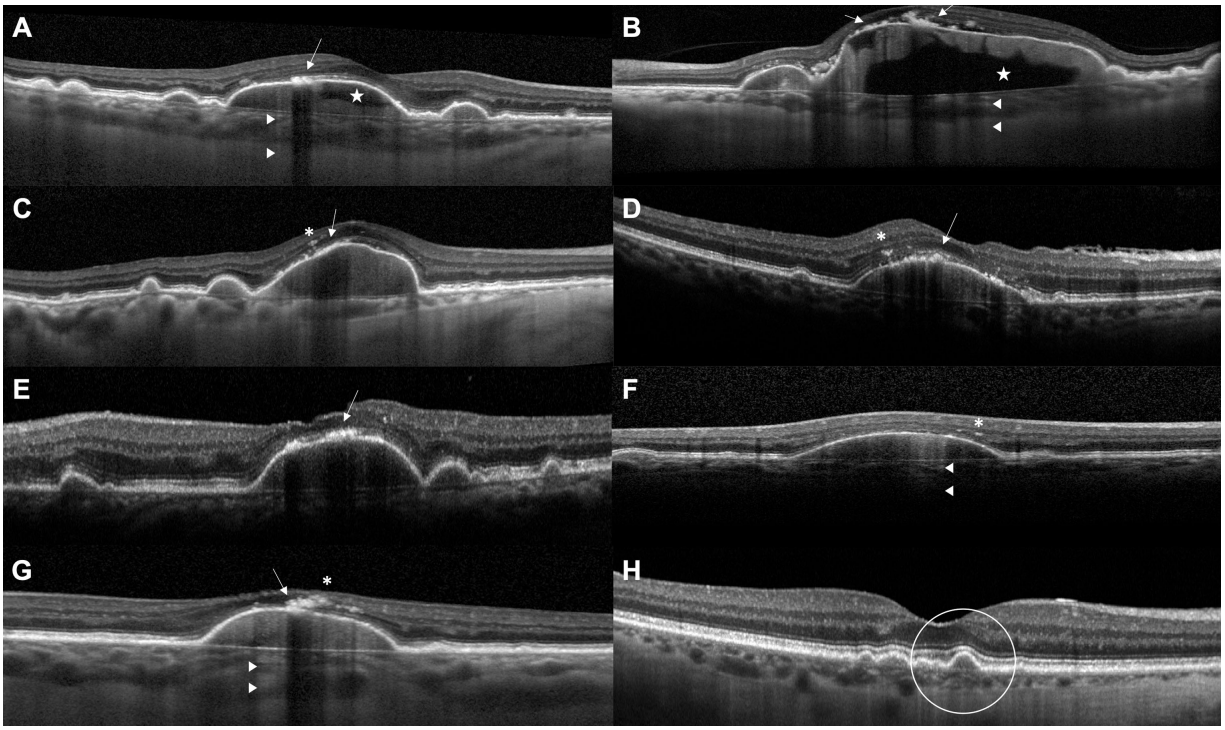

Figure 1. Optical coherence tomography (OCT) B-scans from seven separate cases and one control case of macular drusen. (**A**) OCT B-scan of the right eye illustrates a sub-foveal very large drusen (height 352.9 µm) with early signs of RPE disruption including apical RPE thickening (*white arrow*), apical hyporeflective core (*white star*), diffuse ELM and EZ disruption, and choroidal hypertransmission (*white arrowheads*). (**B**) OCT B-scan of the left eye displays a subfoveal very large druse (height 855.0 µm) with RPE thickening (*white arrows*) and RPE thinning at the apex and between drusen, diffuse EZ/ELM loss, and hyporeflective cores (*white star*), and choroidal hypertransmission (*white arrowheads*). (**C**) OCT B-scan of the right eye illustrates a very large druse (height 430.8 µm) with apical RPE thickening/thinning (*white arrow*) and HRF (*white asterisk*) extending from the apex toward the slope with associated diffuse EZ/ELM disruption. (**D**) OCT B-scan of the right eye displays a very large druse (height 280.9 µm) with apical RPE thickening (*white arrow*) and HRF (*white asterisk*), RPE thinning extending from the apex to the nasal slope, and diffuse EZ/ELM disruption. (**E**) OCT B-scan of the left eye illustrates a very large druse (height 206.2 µm) with apical RPE thickening (*white arrow*) and associated EZ/ELM disruption extending from the apex down the nasal slope. (**F**) OCT B-scan of the right eye displays a very large druse (height 305.3 µm) with apical RPE thinning and HRF (*white asterisk*), diffuse EZ/ELM loss, and choroidal hypertransmission (*white arrowheads*). (**G**) OCT B-scan of the left eye illustrates a subfoveal large druse (height 270.7 µm) with apical evidence of RPE thickening (*white arrow*) and HRF (*white asterisk*) and diffuse ELM and EZ disruption and diffuse choroidal hypertransmission (*white arrowheads*). (**H**) OCT B-scan of the right eye displays a control subfoveal small drusen (*white circle*; height 67.2 µm) without any OCT biomarkers of atrophy.

diffusely (56.4% [53/94]), whereas 41.5% (39/94) of the cases were identified at the apex.

3. RPE thickening or thinning was noted in increasing frequency in the groups with small drusen (0/39 [0%]), intermediate drusen (2/39 [5.1%]), large drusen (12/38 [31.6%]), and very large drusen (30/39 [76.9%]; $P < 0.001$). A post hoc χ^2 test demonstrated that all comparisons, except for the comparison of small versus intermediate drusen ($P = 0.16$) and intermediate and large drusen ($P = 0.003$), were statistically significant. Intergrader Cohen's kappa was 0.77 (95% CI, 0.69–0.84). RPE changes were predominantly located at the apex of the drusen (90.9% [40/44]), although 6.8% (3/44) were located only on the slope.
4. HRF detection also correlated with increasing size of the drusen: small (0/39 [0%]), intermediate (2/39 [5.1%]), large (7/38 [18.4%]), and very large drusen (23/39 [59.0%]; $P < 0.001$). All comparisons were statistically significant except for the comparison of small versus intermediate drusen ($P = 0.32$). The intergrader Cohen's kappa was 0.76 (95% CI, 0.65–0.88).

Investigative Ophthalmology & Visual Science

Table 4. Comparison of Structural and Atrophy Biomarkers Between Largest and Smallest Drusen in Eyes With More Than 1 Druse

	Largest Druse (n = 147)	Control Druse (n = 147)	P Value
Drusen height (μm)	139.2 ± 108.4	62.0 ± 37.5	<0.001
Drusen GHD (μm)	1007.3 ± 879.5	405.0 ± 384.0	<0.001
Choroidal thickness (μm)	219.6 ± 88.7	212.3 ± 93.8	0.20
ELM disruption	84 (57.1)	43 (29.3)	<0.001
EZ disruption	93 (63.3)	40 (27.2)	<0.001
RPE thickening or thinning	43 (29.3)	4 (2.7)	<0.001
HRF	32 (21.8)	3 (2.0)	<0.001
Choroidal hypertransmission	63 (42.9)	19 (12.9)	<0.001
Hyporeflective cores	5 (3.4)	1 (0.7)	0.10

Values are mean ± SD or number (%).

Like RPE changes, HRF were very notably identified only at the apex 100.0% (32/32).

5. Choroidal hypertransmission also showed a statistically significant correlation with increasing drusen size in small drusen (13/39 [33.3%]), intermediate drusen (8/39 [20.5%]), large drusen (16/38 [42.1%]), and very large drusen (29/39 [74.4%]; $P < 0.001$). On post hoc χ^2 testing, all groups were statistically significant different except between small versus intermediate drusen ($P = 0.40$) and intermediate versus large drusen ($P = 0.04$). The intergrader Cohen's kappa was 0.49 (95% CI, 0.38–0.59). Choroidal hypertransmission was primarily identified in a diffuse pattern overlying drusen (71.2% [47/66]) or at the apex (28.8% [19/66]). The lower intergrader Cohen's kappa may be related to shadowing from RPE thickening that makes adjacent areas appear as relative choroidal hypertransmission.
6. The presence of hyporeflective cores was more common in larger drusen. Small, intermediate, and large drusen did not display hyporeflective cores, whereas 12.8% of very large drusen (5/39) were associated with hyporeflective cores ($P = 0.002$). However, on post hoc analysis, no differences remained statistically significant with the conservative Bonferroni correction ($P = 0.02$), likely owing to the limited numbers. Intergrader Cohen's kappa was 1.0 (95% CI, 1.0–1.0). Hyporeflective cores were either identified in a diffuse pattern (3/5 [60%]) or at the apex (2/5 [40%]).

Frequency and Location of OCT Biomarkers of Atrophy Within the Same Eye

To control for variation in AMD severity and choroidal thickness between eyes, the two largest noncontiguous drusen more than 1000 microns apart were identified and choroidal thickness was measured and compared (Table 4). Of the 155 eyes, 147 were enrolled for this control analysis. The largest druse average was 139.2 ± 108.4 μm compared with the control druse average of 62.0 ± 37.5 μm ($P < 0.001$). The GHD of the largest druse was 1007.3 ± 879.5 μm compared with the control druse at 405.0 ± 384.0 μm ($P < 0.001$). There was no difference in the mean choroidal thickness ($P = 0.20$). As with the largest drusen analysis, ELM disruption ($P < 0.001$), EZ disruption ($P < 0.001$), RPE thickening or thinning ($P < 0.001$), HRF ($P < 0.001$), and choroidal hypertransmission ($P < 0.001$) were all statistically significantly more frequent in the largest druse compared with the control druse. However, hyporeflective cores was not statistically significant between largest druse versus control druse ($P = 0.10$).

Relationship Between Height and Diameter of Drusen

Logistic regressions are summarized in Figure 2. Drusen height was more significantly correlated with predictive biomarkers of atrophy than drusen GHD. Drusen height was significantly correlated with every OCT biomarker of atrophy. Disruption of the ELM (rho = 0.67; $P = 0.003$), disruption of the EZ (rho = 0.65; $P < 0.001$), RPE thickening and thinning (rho = 0.63; $P < 0.001$), intraretinal HRF (rho = 0.54; $P = 0.008$), choroidal hypertransmission (rho = 0.30; $P = 0.009$), and presence of hyporeflective cores (rho = 0.28, $P < 0.001$) showed statistically positive correlations with drusen height independent of drusen GHD, while controlling for bilateral eye enrollment. By contrast, the only statistically significant correlation between drusen GHD was presence of HRF (rho = 0.52; $P = 0.001$). This analysis indicates that the significant correlations of drusen size with OCT predictors of atrophy may be driven by drusen height.

Discussion

In this cross-sectional OCT study, we showed that drusen height, more importantly than GHD, is correlated with the presence of OCT predictors of atrophy, including ELM and EZ disruption, RPE thickening and thinning, intraretinal HRF, choroidal transmission, and the presence of hyporeflective cores. We found a linear correlation between drusen height and the presence of OCT biomarkers of atrophy and showed that taller drusen, as measured by maximum drusen height, correlated with a significantly greater frequency of early signs of atrophy. This study expands on prior studies that have identified drusen height as a risk factor for atrophy, but our study is the first to suggest that drusen height may be a more important predictor than drusen GHD and that this risk may relate to the development of RPE impairment and disruption as a factor of RPE distance from the choroid.[8,10–16] Moreover, our study showed that OCT biomarkers of atrophy, such as RPE disruption and HRF, are predominantly located at the apex of the drusen, again emphasizing the importance of RPE separation distance from the underlying choroid. The significant correlations of drusen size with OCT predictors of atrophy, therefore, may be driven predominantly by drusen height and separation distance from the choroid causing RPE disruption and, ultimately, RPE atrophy. We speculate that the maximum separation distance of the

Investigative Ophthalmology & Visual Science

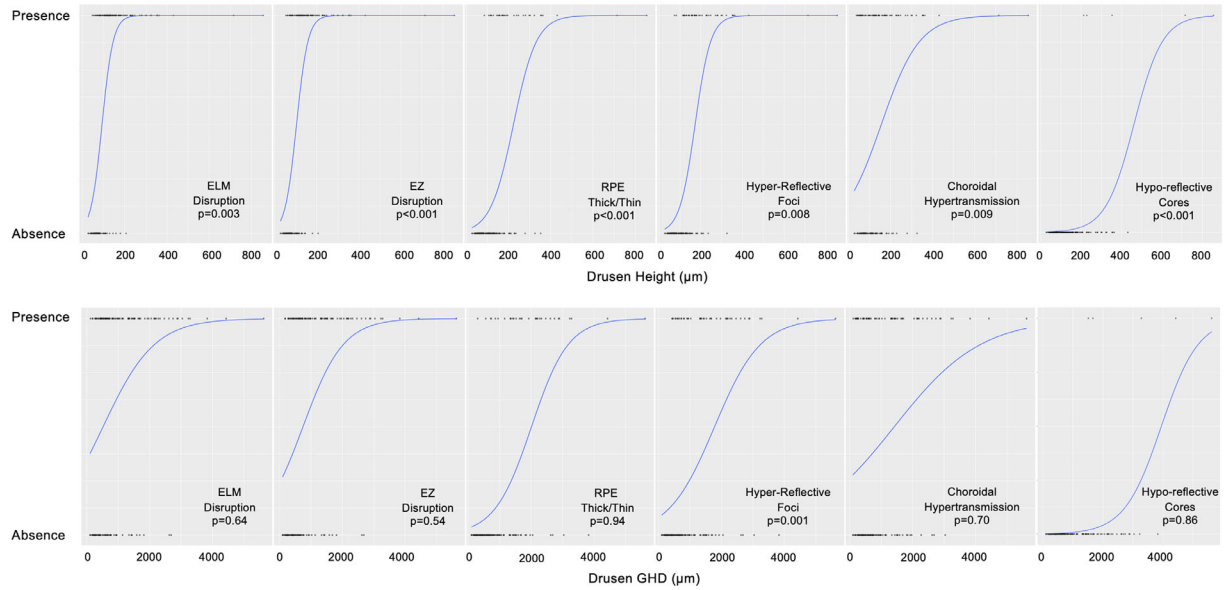

Figure 2. Summary of the logistic regression showing the probability of having a predictive OCT biomarker of atrophy as correlated with increasing drusen height or GHD. The *y*-axis is the presence or absence of the OCT biomarker and the *x*-axis is drusen height (*top*) or GHD (*bottom*) in microns. Logistic regression between all OCT biomarkers of atrophy and drusen height were statistically significant while GHD was only statistically significant with HRF.

RPE to the choroid leading to RPE impairment and disruption may be the result of RPE ischemia, but this point requires future validation.

Curcio et al.[5] have studied the OCT and corresponding histopathological stages before atrophy in AMD and have noted morphological changes in the RPE predating frank atrophy. Specifically, Curcio et al. noted the following morphological alterations at the apex of a drusenoid PED: RPE cells dissociate and aggregate along the RPE (thickened RPE on OCT) and then migrate anteriorly into the retina (intraretinal HRF on OCT) leading to RPE thinning and the development of vertical streaks of hypertransmission (choroidal hypertransmission on OCT).[5] In a separate study of drusenoid PED, 76.5% of patients with disruptions in the RPE and basal lamina were noted to be at the apex.[15] The cause of RPE activation is unclear. RPE breakdown may be incited by greater separation distance of the RPE from the choroid. This factor may explain the apical location of the identified OCT precursors, higher frequency of biomarkers in large drusen, and positive correlation of drusen height with the presence of atrophy biomarkers and with RPE atrophy.

In further support of RPE impairment and failure resulting from greater separation distance from the underlying choroid, subretinal fluid and acquired vitelliform lesions have been described in association with large drusenoid PED. Hilely et al.[6] analyzed patients with subretinal fluid in non-neovascular AMD and found that the presence of subretinal fluid was commonly located at the apex of the drusenoid PED, was associated with many OCT features of atrophy (e.g., focal RPE thickening, HRF), and predated progression to frank atrophy. Similarly, RPE pump failure may partly explain why persistent subretinal fluid can complicate 15% to 45% of eyes despite monthly anti-VEGF injections in the CATT, VIEW, and HAWK/HARRIER studies.[17–19] This finding reinforces the importance of understanding the role of RPE impairment in both non-neovascular and neovascular AMD because RPE pump failure and phagocytic dysfunction can be factors in both the development of non-neovascular fluid and acquired vitelliform lesions, respectively.

This study is limited by its retrospective and cross-sectional study design. Drusen are dynamic and can increase and decrease in size, although the decrease and collapse of large drusen and drusenoid PED is typically a stage before the development of RPE atrophy and cRORA. We captured drusen only in eyes without any evidence of cRORA. An early time point was captured for each case to identify early biomarkers of atrophy; however, additional longitudinal analysis is important to validate the outcomes of this study. Our strict inclusion criteria decreases the generalizability of our results to an overall AMD cohort. We excluded eyes with pseudodrusen or subretinal drusenoid deposits, which have been shown to have a different pathogenesis of development than large or very large macular drusen.[20] Drusen were analyzed within the entire OCT macular cube but differences in EZ, ELM, and RPE thicknesses differ across the macula, which may decrease or increase their susceptibility for disruption. Drusen volume incorporates both GHD and height and, therefore, may provide the most informative quantitative risk factor of atrophy. However, drusen volume analysis is not ubiquitously available to clinicians and requires high-density OCT B-scans, which can be a more cumbersome approach. Drusen height may provide a more practical measure of drusen risk for clinicians, but the accuracy of peak height detection can be affected by the density of the volume scan, a further limitation of this study. The lack of correction based on patient biometry preferentially affects horizontal measurements, decreasing the reliability of these values.[21] Therefore, the actual dimensions of the GHD are nominal and may not reflect the true GHD. This factor, however, does not affect the statistical comparison between the largest and control druse, used as a control analysis for the study because they are subject to the same error. In

addition, this finding further supports drusen height as a more reliable index than GHD. Last, findings from this study only confer association or correlation, but not causation. Future studies with oxygen tension and RPE function at the apex of drusen could confirm or refute our finding that RPE separation from the choroid, possibly leading to RPE ischemia, is the critical factor driving RPE impairment and breakdown.

In conclusion, this study demonstrated the increased frequency and positive linear correlation of predictive OCT biomarkers of atrophy with the height of drusen. Greater drusen height was more significantly associated with the presence of ELM and EZ disruption, RPE thinning or thickening, intraretinal HRF, choroidal transmission, and the presence of hyporeflective cores than drusen diameter. This finding may be explained by the increased separation distance of the RPE from the underlying choroid and may explain why early biomarkers of atrophy are noted most frequently at the apex. The identification of AMD eyes with greater drusen height may be appropriate targets for early intervention therapeutics to prevent atrophy and vision loss.

Acknowledgments

Disclosure: **A. Au**, None; **A. Santina**, None; **N, Abraham**, None; **M.F. Levin**, None; **G. Corradetti**, None; **S. Sadda**, Amgen (C), Allergan (C), Novartis (C, S), Roche/Genentech (C), Regeneron (C), Bayer (C), 4DMT (C), Astellas (C), Apellis (C), Iveric (C), Optos (F, C, S), Centervue (F, C), Heidelberg (F, C, S), Nidek (S), Topcon (S), Carl Zeiss Meditec (S); **D. Sarraf**, Amgen (C, F, R), Bayer (C, R), Boehringer (F), Genetech (C, F, R), Novartis (C, F, R), Iveric Bio (C, R), Heidelberg Engineering (F), Optovue (F, I, C, S), Topcon (F), Regeneron (F, R)

References

1. Age-Related Eye Disease Study Research Group. The age-related eye disease study system for classifying age-related macular degeneration from stereoscopic color fundus photographs: the age-related eye disease study report number 6. *Am J Ophthalmol*. 2001;132:668–681.
2. Klein R, Davis MD, Magli YL, et al. The Wisconsin Age-related Maculopathy Grading System. *Ophthalmology*. 1991;98:1128–1134.
3. Cukras C, Agrón E, Klein ML, et al. Natural history of drusenoid pigment epithelial detachment in age-related macular degeneration: Age-Related Eye Disease Study Report No. 28. *Ophthalmology*. 2010;117:489–499.
4. Jaffe GJ, Chakravarthy U, Freund KB, et al. Imaging features associated with progression to geographic atrophy in age-related macular degeneration. *Ophthalmol Retin*. 2020;5:855–867.
5. Curcio CA, Zanzottera EC, Ach T, et al. Activated retinal pigment epithelium, an optical coherence tomography biomarker for progression in age-related macular degeneration. *Invest Ophthalmol Vis Sci*. 2017;58:BIO211–BIO226.
6. Hilely A, Au A, Freund KB, et al. Non-neovascular age-related macular degeneration with subretinal fluid. *Br J Ophthalmol*. 2020;105:1415–1420. bjophthalmol-2020-317326.
7. Ouyang Y, Heussen FM, Hariri A, et al. Optical coherence tomography-based observation of the natural history of drusenoid lesion in eyes with dry age-related macular degeneration. *Ophthalmology*. 2013;120:2656–2665.
8. Sadda SR, Guymer R, Holz FG, et al. Consensus definition for atrophy associated with age-related macular degeneration on OCT. *Ophthalmology*. 2018;125:537–548.
9. Schindelin J, Arganda-Carreras I, Frise E, et al. Fiji: an open-source platform for biological-image analysis. *Nat Methods*. 2012;9:676–682.
10. Christenbury JG, Folgar FA, O'Connell RV, et al. Progression of intermediate age-related macular degeneration with proliferation and inner retinal migration of hyperreflective foci. *Ophthalmology*. 2013;120:1038–1045.
11. Schmidt-Erfurth U, Waldstein SM, Klimscha S, et al. Prediction of individual disease conversion in early AMD using artificial intelligence. *Invest Ophthalmol Vis Sci*. 2018;59:3199.
12. Ferrara D, Silver RE, Louzada RN, et al. Optical coherence tomography features preceding the onset of advanced age-related macular degeneration. *Invest Ophthalmol Vis Sci*. 2017;58:3519.
13. Ouyang Y, Heussen FM, Hariri A, et al. Optical coherence tomography–based observation of the natural history of drusenoid lesion in eyes with dry age-related macular degeneration. *Ophthalmology*. 2013;120:2656–2665.
14. Balaratnasingam C, Messinger JD, Sloan KR, et al. Histologic and optical coherence tomographic correlates in drusenoid pigment epithelium detachment in age-related macular degeneration. *Ophthalmology*. 2017;124:644–656.
15. Balaratnasingam C, Yannuzzi LA, Curcio CA, et al. Associations between retinal pigment epithelium and drusen volume changes during the lifecycle of large drusenoid pigment epithelial detachments. *Invest Ophthalmol Vis Sci*. 2016;57:5479.
16. Mrejen S, Sarraf D, Mukkamala SK, Freund KB. Multimodal imaging of pigment epithelial detachment: a guide to evaluation. *Retina*. 2013;33:1735–1762.
17. Core JQ, Pistilli M, Daniel E, et al. Predominantly persistent subretinal fluid in the comparison of age-related macular degeneration treatments trials. *Ophthalmol Retin*. 2021;5:962–974.
18. Jaffe GJ, Kaiser PK, Thompson D, et al. Differential response to anti-VEGF regimens in age-related macular degeneration patients with early persistent retinal fluid. *Ophthalmology*. 2016;123:1856–1864.
19. Sharma A, Kumar N, Parachuri N, et al. Brolucizumab and fluid in neovascular age-related macular degeneration (n-AMD). *Eye*. 2020;34:1310–1312.
20. Zweifel SA, Spaide RF, Curcio CA, et al. Reticular pseudodrusen are subretinal drusenoid deposits. *Ophthalmology*. 2010;117:303–312.e1.
21. Odell D, Dubis AM, Lever JF, et al. Assessing errors inherent in OCT-derived macular thickness maps. *J Ophthalmol*. 2011;2011:1–9.